Chapter Contents

Chapter Glossary

(ADCS)	Attitude Determination and Control System
(CoCom)	Coordinating Committee for Multilateral Export Controls
(COTS)	Commercial-off-the-Shelf
(DOF)	Degrees of Freedom
(DSAC)	Deep Space Atomic Clock
(DSN)	Deep Space Network
(EAR)	Export Administration Regulations
(FOGs)	Fiber Optic Gyros
(GNC)	Guidance, Navigation & Control
(GSO)	Geo-stationary Orbit
(USAF)	U.S. Air Force
(HCI)	Horizon Crossing Indicators
(IMUs)	Inertial Measurement Units
(JPL)	Jet Propulsion Laboratory
(LMRST)	Low Mass Radio Science Transponder
(MarCO)	Mars Cube One
(PMSM)	Permanent-magnet Synchronous Motor
(SDST)	Small Deep Space Transponder
(SWaP)	Size, weight, and power
(TLE)	Two-Line Element
(TRL)	Technology Readiness Level

5.0 Guidance, Navigation & Control

5.1 Introduction

The Guidance, Navigation & Control (GNC) subsystem includes both the components used for position determination and the components used by the Attitude Determination and Control System (ADCS). In Earth orbit, onboard position determination can be provided by a Global Positioning System (GPS) receiver. Alternatively, ground-based radar tracking systems can also be used. If onboard knowledge is required, then these radar observations can be uploaded and paired with a suitable propagator. Commonly, the U.S. Air Force (USAF) publishes Two-Line Element sets (TLE) (1), which are paired with a SGP4 propagator (2). In deep space, position determination is performed using the Deep Space Network (DSN) and an onboard radio transponder (3). There are also optical technologies being developed that use celestial bodies such as planets and pulsars to provide position data (26).

Using SmallSats in cislunar space and beyond requires a slightly different approach than the GNC subsystem approach in low-Earth orbit. Use of the Earth's magnetic field, for example, is not possible in these missions, and alternate ADCS designs and methods must be carefully considered. Two communication relay CubeSats (Mars Cube One, MarCO) successfully demonstrated such interplanetary capability during the 2018 Insight mission to Mars (4). This interplanetary mission demonstrated both the capability of this class of spacecraft and the GNC fine pointing design for communication in deep space.

ADCS includes sensors to determine attitude and attitude rate, such as star trackers, sun sensors, horizon sensors, magnetometers, and gyros. In addition, the ADCS is often used to control the vehicle during trajectory correction maneuvers and, using accelerometers, to terminate maneuvers when the desired velocity change has been achieved. Actuators are designed to change a spacecraft's attitude and to impart velocity change during trajectory correction maneuvers. Common spacecraft actuators include magnetic torquers, reaction wheels, and thrusters. There are many attitude determination and control architectures and algorithms suitable for use in small spacecraft (5).

Miniaturization of existing technologies is a continuing trend in small spacecraft GNC. While three-axis stabilized, GPS-equipped, 100 kg class spacecraft have been flown for decades, it has only been in the past few years that such technologies have become available for micro- and nano-class spacecraft. Table 5-1 summarizes the current state-of-the-art of performance for GNC subsystems in small spacecraft. Performance greatly depends on the size of the spacecraft and values will range for nano- to micro-class spacecraft.

The information described below is not intended to be exhaustive but provides an overview of current state-of-the-art technologies and their development status for a particular small spacecraft subsystem. It should be noted that Technology Readiness Level (TRL) designations may vary with changes specific to payload, mission requirements, reliability considerations, and/or the environment in which performance was demonstrated. Readers are highly encouraged to reach out to companies for further information regarding the performance and TRL of described technology. There is no intention of mentioning certain companies and omitting others based on their technologies or relationship with NASA.

Table 5-1: State-of-the-Art GNC Subsystems		
Component	**Performance**	**TRL**
Reaction Wheels	0.00023 – 0.3 Nm peak torque, 0.0005 – 8 N m s storage	7-9
Magnetic Torquers	0.15 A m^2 – 15 A m^2	7-9
Star Trackers	8 arcsec pointing knowledge	7-9
Sun Sensors	0.1° accuracy	7-9
Earth Sensors	0.25° accuracy	7-9
Inertial Sensors	Gyros: 0.15° h^{-1} bias stability, 0.02° $h^{-1/2}$ ARW Accels: 3 μg bias stability, 0.02 (m s^{-1})/$h^{-1/2}$ VRW	7-9
GPS Receivers	1.5 m position accuracy	7-9
Integrated Units	5 – 0.002° pointing capability	7-9
Atomic Clocks	10 – 150 Frequency Range (MHz)	5-6
Deep Space Navigation	Bands: X, Ka, S, and UHF	7-9

5.2 State-of-the-Art – GNC Subsystems

5.2.1 Integrated Units

Integrated units combine multiple different attitude and navigation components to provide a simple, single-component solution to a spacecraft's GNC requirements. Typical components included are reaction wheels, magnetometers, magnetic torquers, and star trackers. The systems often include processors and software with attitude determination and control capabilities. Table 5-2 describes some of the integrated systems currently available. Blue Canyon Technologies' XACT (figure 5.1) flew on the NASA-led missions MarCO and ASTERIA, both of which were 6U platforms, and have also flown on 3U missions (MinXSS was deployed from NanoRacks in February 2016).

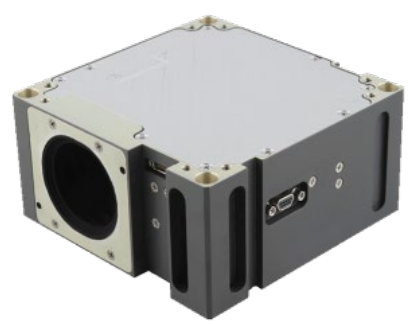

Figure 5.1: BCT XACT Integrated ADCS Unit. Credit: Blue Canyon Technologies.

Table 5-2. Currently Available Integrated Systems							
Manufacturer	**Model**	**Mass (kg)**	**Actuators**	**Sensors**	**Processor**	**Pointing Accuracy**	**TRL**
Arcsec	Arcus ADC	0.715	3 reaction wheels 3 magnetic torquers	1 star tracker 3 gyros 6 photodiodes 3 magnetometers	Yes	0.1°	7-9
Berlin Space Technologies / Hyperion Technologies	iADCS-200	0.400	3 reaction wheels 3 magnetic torquers	1 star tracker 3 gyros, 1 magnetometer, 1 accelerometer	Yes	1°	7-9
Berlin Space Technologies / Hyperion Technologies	iADCS-400	1.7	3 reaction wheels 3 magnetic torquers	1 star tracker, optional IMU	Yes	<1°	7-9
Blue Canyon Technologies	XACT-15	0.885	3 reaction wheels 3 magnetorquers	1 star tracker 3-axis magnetometer	Yes	0.007°	7-9
Blue Canyon Technologies	XACT-50	1.230	3 reaction wheels 3 magnetorquers	1 star tracker 3-axis magnetometer	Yes	0.007°	7-9
Blue Canyon Technologies	XACT-100	1.813	3 reaction wheels 3 magnetorquers	1 star tracker 3-axis magnetometer	Yes	0.007°	7-9
Blue Canyon Technologies	Flexcore	configuration dependent	3 – 4 reaction wheels 3 magnetorquers	1 star tracker 3-axis magnetometer	Yes	0.007°	7-9
CubeSpace	CubeADCS 3-Axis Small	0.55	3 reaction wheels 3 magnetorquers	10 coarse sun sensors 2 fine sun/earth sensors 1 magnetometer	Yes	<1°	7-9

CubeSpace	CubeADCS 3-Axis Small with Star Tracker	0.61	3 reaction wheels 3 magnetorquers	10 coarse sun sensors 2 fine sun/earth sensors 1 magnetometer 1 star tracker	Yes	<0.5°	7-9
CubeSpace	CubeADCS 3-Axis Medium	0.79	3 reaction wheels 3 magnetorquers	10 coarse sun sensors 2 fine sun/earth sensors 1 magnetometer	Yes	<1°	7-9
CubeSpace	CubeADCS 3-Axis Medium with Star Tracker	0.84	3 reaction wheels 3 magnetorquers	10 coarse sun sensors 2 fine sun/earth sensors 1 magnetometer 1 star tracker	Yes	<0.5°	7-9
CubeSpace	CubeADCS 3-Axis Large	1.1	3 reaction wheels 3 magnetorquers	10 coarse sun sensors 2 fine sun/earth sensors 1 magnetometer	Yes	<1°	7-9
CubeSpace	CubeADCS 3-Axis Large with Star Tracker	1.15	3 reaction wheels 3 magnetorquers	10 coarse sun sensors 2 fine sun/earth sensors 1 magnetometer 1 star tracker	Yes	<0.5°	7-9
CubeSpace	CubeADCS Y-Momentum	0.3	3 reaction wheels 3 magnetic torquers	10 coarse sun sensors 1 magnetometer	Yes	<5°	7-9

5.2.2 Reaction Wheels

Miniaturized reaction wheels provide small spacecraft with a three-axis precision pointing capability and must be carefully selected based on several factors including the mass of the spacecraft and the required rotation performance rates. Reaction wheels provide torque and momentum storage along the wheel spin axis and require the spacecraft to counter-rotate around the spacecraft center of mass due to conservation of angular momentum from the wheel spin direction. Table 5-3 lists a selection of high-heritage miniature reaction wheels. Except for three units, all the reaction wheels listed have spaceflight heritage. For full three-axis control, a spacecraft requires three wheels. However, a four-wheel configuration is often used to provide fault tolerance (6). Due to parasitic external torques, reaction wheels need to be periodically desaturated using an actuator that provides an external torque, such as thrusters or magnetic torquers (7).

In addition, the multiple reaction wheels are often assembled in a “skewed” or angled configuration such that there exists a cross-coupling of torques with two or more reaction wheels. While this reduces the torque performance in any single axis, it allows a redundant, albeit reduced, torque capability in more than one axis. The result is that should any single reaction wheel fail, one or more reaction wheels are available as a reduced-capability backup option.

Table 5-3 High Heritage Miniature Reaction Wheels

Manufacturer	Model	Mass (kg)	Peak Power (W)	Peak Torque (Nm)	Momentum Capacity (Nms)	# Wheels	Radiation Tolerance (krad)	TRL
Berlin Space Technologies	RWA05	1.700	0.5	0.020	0.5	1	30	7-9
Blue Canyon Technologies	RWP015	0.130	1	0.004	0.015	1	Unk	7-9
Blue Canyon Technologies	RWp050	0.240	1	0.007	0.050	1	Unk	7-9
Blue Canyon Technologies	RWp100	0.330	1	0.007	0.100	1	Unk	7-9
Blue Canyon Technologies	RWp500	0.750	6	0.025	0.500	1	Unk	7-9
Blue Canyon Technologies	RW1	0.950	9	0.100	1.000	1	Unk	7-9
Blue Canyon Technologies	RW4	3.200	10	0.250	4.000	1	Unk	7-9
Blue Canyon Technologies	RW8	4.400	10	0.250	8.000	1	Unk	7-9
CubeSpace	CubeWheel Small	0.060	0.65	0.00023	0.00177	1	24	7-9
CubeSpace	CubeWheel Small+	0.090	2.3	0.0023	0.0036	1	24	7-9
CubeSpace	CubeWheel	0.150	2.3	0.001	0.0108	1	24	7-9

	Medium							
CubeSpace	CubeWheel Large	0.225	4.5	0.0023	0.0306	1	24	7-9
GomSpace	NanoTorque GSW-600	0.940	0.3	0.0015	0.019	1	Unk	Unk
Hyperion Technologies	RW210	0.48	0.8	0.0001	0.006	1	36	7-9
Hyperion Technologies	RW400	0.375	1.9	0.012	0.050	1	36	7-9
NanoAvionics	RWO	0.137	3.25	0.003	0.020	1	20	7-9
NanoAvionics	4RWO	0.665	6	0.006	0.037	4	20	7-9
NewSpace Systems	NRWA-T005	1.2	0.4	0.01	0.050	1	10	7-9
NewSpace Systems	NRWA-T065	1.55	0.8	0.02	0.65	1	10	7-9
NewSpace Systems	NRWA-T2	2.2	1.08	0.09	2	1	10	7-9
Sinclair Interplanetary	RW-0.03	0.185	1.8	0.002	0.040	1	20	7-9
Sinclair Interplanetary	RW-0.003	0.050	Unk	0.001	0.005	1	10	5-6
Sinclair Interplanetary	RW-0.01	0.120	1.05	0.001	0.018	1	20	7-9
Sinclair Interplanetary	RW3-0.06	0.226	23.4	0.020	0.180	1	20	7-9
Sinclair Interplanetary	RW4-0.2	0.6	Unk	0.1	0.2	1	60	7-9
Sinclair Interplanetary	RW4-0.4	0.77	Unk	0.1	0.4	1	60	7-9
Sinclair Interplanetary	RW4-1.0	1.38	45	0.1	1	1	60	7-9
Vectronic Aerospace	VRW-A-1	1.900	110	0.090	6.000	1	20	Unk
Vectronic Aerospace	VRW-B-2	1.000	45	0.020	0.200	1	20	Unk
Vectronic Aerospace	VRW-C-1	2.3	45	0.020	1.20	1	20	Unk
Vectronic Aerospace	VRW-D-2	2	65	0.05	2.0	1	20	Unk

Vectronic Aerospace	VRW-D-6	3	110	0.09	6	1	20	Unk

5.2.3 Magnetic Torquers

Magnetic torquers provide control torques perpendicular to the local external magnetic field. Table 5-4 lists a selection of high heritage magnetic torquers and figure 5.3 illustrates some of ZARM Technik's product offerings. Magnetic torquers are often used to remove excess momentum from reaction wheels. As control torques can only be provided in the plane perpendicular to the local magnetic field, magnetic torquers alone cannot provide three-axis stabilization.

Figure 5.3: Magnetorquers for micro satellites. Credit: ZARM Technik.

Use of magnetic torquers beyond low-Earth orbit and in interplanetary applications need to be carefully investigated since their successful operation is dependent on a significant local external magnetic field. This magnetic field may or may not be available in the location and environment for that mission and additional control methods will be required during transit.

Table 5-4. High Heritage Magnetic Torquers							
Manufacturer	**Model**	**Mass (kg)**	**Power (W)**	**Peak Dipole (A m²)**	**# Axes**	**Radiation Tolerance (krad)**	**TRL**
CubeSpace	CubeTorquer Small	0.028	0.42	0.24	1	24	7-9
CubeSpace	CubeTorquer Medium	0.036	0.37	0.66	1	24	7-9
CubeSpace	CubeTorquer Large	0.072	0.37	1.90	1	24	7-9
CubeSpace	CubeTorquer Coil(Single)	0.046	0.31	0.13	1	24	7-9
CubeSpace	CubeTorquer Coil(Double)	0.074	0.64	0.27	1	24	7-9
GomSpace	Nano Torque GST-600	0.156	Unk	0.31 – 0.34	3	Unk	Unk
GomSpace	NanoTorque Z-axis Internal	0.106	Unk	0.139	1	Unk	Unk
ISISPACE	Magnetorquer Board	0.196	1.2	0.20	3	Unk	7-9
MEISEI	Magnetic Torque Actuator for Spacecraft	0.5	1	12	1	Unk	7-9
Hyperion Technologies	MTQ800	0.395	3	15	1	Unk	7-9
NanoAvionics	MTQ3X	0.205	0.4	0.30	3	20	7-9

NewSpace Systems	NCTR-M003	0.030	0.25	0.29	1	Unk	7-9
NewSpace Systems	NCTR-M012	0.053	0.8	1.19	1	Unk	7-9
NewSpace Systems	NCTR-M016	0.053	1.2	1.6	1	Unk	7-9
Sinclair Interplanetary	TQ-40	0.825	Unk	48.00	1	Unk	7-9
Sinclair Interplanetary	TQ-15	0.400	Unk	19.00	1	Unk	7-9
ZARM	MT0.2-1	0.005	0.25	0.2	1	Unk	7-9
ZARM	MT1-1	0.060	0.23	1	1	Unk	7-9
ZARM	MT2-1	0.2	0.5	2	1	Unk	7-9
ZARM	MT4-1	0.15	0.6	4	1	Unk	7-9
ZARM	MT5-1	0.19	0.73	5	1	Unk	7-9
ZARM	MT5-2	0.3	0.77	5	1	Unk	7-9
ZARM	MT6-2	0.3	0.48	6	1	Unk	7-9
ZARM	MT7-2	0.4	0.9	7	1	Unk	7-9
ZARM	MT10-1-01	0.35	0.53	10	1	Unk	7-9
ZARM	MT10-2-H	0.37	1	10	1	Unk	7-9
ZARM	MT15-1	0.45	1.1	15	1	Unk	7-9

5.2.4 Thrusters

Thrusters used for attitude control are described in Chapter 4: In-Space Propulsion. Pointing accuracy is determined by minimum impulse bit, and control authority by thruster force.

5.2.5 Star Trackers

A star tracker can provide an accurate, standalone estimate of three-axis attitude by comparing a digital image captured with a focal plane array detector to an onboard star catalog (8). Star trackers typically identify and track multiple stars and provide three-axis attitude (and often attitude rate) several times a second, usually provided as a quaternion. Table 5-5 lists some models suitable for use on small spacecraft. For example, Arcsec's Sagitta Star Tracker was launched on the SIMBA cubesat in 2020.

Table 5-5. Star Trackers Suitable for Small Spacecraft								
Manufacturer	**Model**	**Mass (kg)**	**Power (W)**	**FOV**	**Cross axis accuracy (3s)**	**Twist accuracy (3s)**	**Radiation Tolerance (krad)**	**TRL**
Redwire Space	Star Tracker	0.475	2	14x19	10/27"	51"	75	7-9
Arcsec	Sagitta	0.26	1.2	25.4°	6	30	20	7-9
Arcsec	Twinkle	0.04	0.6	10.4°	30	180	Unk	7-9
Ball Aerospace	CT-2020	3.000	8	Unk	1.5"	1"	Unk	5-6
Berlin Space Technologies / Hyperion Technologies	ST200	0.040	0.65	22°	30"	200"	11	7-9
Berlin Space Technologies / Hyperion Technologies	ST400	0.250	0.67	15°	15"	150"	11	7-9
Blue Canyon Technologies	Standard NST	0.350	1.5	10° x 12°	6"	40"	Unk	7-9
Blue Canyon Technologies	Extended NST	1.300	1.5	10° x 12°	6"	40"	Unk	7-9
Creare	UST	0.840	Unk	Unk	7"	15"	Unk	5-6
CubeSpace	CubeStar	0.055	0.264	42° diameter	55.44"	77.4	19	7-9
Danish Technical University	MicroASC	0.425	1.9	Unk	Unk	Unk	Unk	7-9
Leonardo	Spacestar	1.600	6	20° x 20°	7.7"	10.6"	Unk	7-9
NanoAvionics	ST-1	0.108	1.2	21° full-cone	8"	50"	20	7-9

Sinclair Interplanetary	ST-16RT2	0.185	1	8° half-cone	5"	55"	Unk	7-9
Sodern	Auriga-CP	0.210	1.1	Unk	2"	11"	Unk	7-9
Sodern	Hydra-M	2.75	8	Unk	Unk	Unk	Unk	5-6
Sodern	Hydra-TC	5.3	8	Unk	Unk	Unk	Unk	5-6
Solar MEMS Technologies	STNS	0.14	1.4	13° x 18°	40"	70"	20	7-9
Space Micro	MIST	0.520	4	14.5°	15"	105"	30	7-9
Space Micro	μSTAR-100M	1.800	5	Unk	15"	105"	100	Unk
Space Micro	μSTAR-200M	2.100	10	Unk	15"	105"	100	Unk
Space Micro	μSTAR-200H	2.700	10	Unk	3"	21"	100	Unk
Space Micro	μSTAR-400M	3.300	18	Unk	15"	105"	100	Unk
Terma	T1	0.923	0.75	20° circular	2.2"	9"	100	5-6
Terma	T3	0.35	.5	20° circular	2.6"	10"	8	5-6
Vectronic Aerospace	VST-41MN	0.900	2.5	14° x 14°	27"	183"	20	7-9
Vectronic Aerospace	VST-68M	0.470	3	14° x 14°	7.5"	45"	20	Unk

5.2.6 Magnetometers

Magnetometers provide a measurement of the local magnetic field and this measurement can be used to provide both estimates of attitude (9). The vast majority of CubeSats use commercial-off-the-shelf (COTS) magnetometers and improve their performance with software. Table 5-6 provides a summary of some three-axis magnetometers available for small spacecraft, one of which is illustrated in figure 5.4.

Figure 5.4: NSS Magnetometer. Credit: NewSpace Systems.

Table 5-6. Three-axis Magnetometers for Small Spacecraft

Manufacturer	Model	Mass (kg)	Power (W)	Resolution (nT)	Orthogonality	Radiation Tolerance (krad)	TRL
GomSpace	NanoSense M315	0.008	Unk	Unk	Unk	Unk	7-9
Hyperion Technologies	MM200	0.012	0.01	Unk	Unk	30	7-9
MEISEI	3-Axis Magnetometer for Small Satellite	0.220	1.5	Unk	1°	Unk	7-9
NewSpace Systems	NMRM-Bn25o485	0.085	0.75	8	1°	10	7-9
SpaceQuest	MAG-3	0.100	Voltage Dependent	Unk	1°	10	7-9
ZARM	Analogue High-Rel Fluxgate Magnetometer FGM-A-75	0.33	0.75	Unk	1°	50	7-9
ZARM	Digital AMR Magnetometer AMR-RS422	0.06	0.3	Unk	1°	Unk	7-9
ZARM	Digital AMR Magnetometer AMR-D-100-EFRS485	0.1	0.2	Unk	1°	30	5-6

5.2.7 Sun Sensors

Sun sensors are used to estimate the direction of the Sun in the spacecraft body frame. Sun direction estimates can be used for attitude estimation, though to obtain a three-axis attitude estimate at least one additional independent source of attitude information is required (e.g., the Earth nadir vector or the direction to a star). Because the Sun is easily identifiable and extremely bright, Sun sensors are often used for fault detection and recovery. However, care must be taken to ensure the Moon or Earth’s albedo is not inadvertently misidentified as the sun.

Figure 5.5: Redwire Coarse Sun Sensor Detector (Cosine Type). Credit: Redwire Space

There are several types of Sun sensors which operate on different principles, but the most common types for small spacecraft are cosine detectors and quadrant detectors. Quadrant detectors appear to be gaining popularity in the CubeSat world due to their compact size and low cost.

Cosine detectors are photocells. Their output is the current generated by the cell, which is (roughly) proportional to the cosine of the angle between the sensor boresight and the Sun. For that reason, at least two cosine detectors (pointing in different directions) are needed to estimate the direction to the Sun and typically four are used to obtain an unambiguous solution and for additional sky coverage. Cosine detectors (e.g., figure 5.5) are inexpensive, low-mass, simple and reliable devices, but their accuracy is typically limited to a few degrees and they do require analog-to-digital converters.

Quadrant detectors. Quadrant sun sensors typically operate by shining sun light through a square window onto a 2 x 2 array of photodiodes. The current generated by each photodiode is a function of the direction of the sun relative to the sensor boresight. The measured currents from all four cells are then combined mathematically to produce the angles to the sun.

Examples of small spacecraft sun sensors are described in table 5-7.

Table 5-7. Small Spacecraft Sun Sensors										
Manufacturer	**Model**	**Sensor Type**	**Mass (kg)**	**Peak Power (W)**	**Analog or Digital**	**FOV**	**Accuracy (3s)**	**# Measurement Angles**	**Radiation Tolerance (krad)**	**TRL**
Redwire Space	Coarse Analog Sun Sensor	Coarse Analog Sun Sensor	0.045	0	Analog	±40° (Can be modified to meet specific FOV requirements)	±1°	1	>100	7-9
Redwire Space	Coarse Sun Sensor (Cosine Type)	Coarse Sun Sensor (Cosine Type)	0.010	0	Analog	APPROXIMATE COSINE, CONICAL SYMMETRY	±2° to ±5°	Depends on configuration	>100	7-9
Redwire Space	Coarse Sun Sensor Pyramid	Coarse Sun Sensor Pyramid	0.13	0	Analog	2π STERADIAN PLUS	±1° to ±3°	2	>100	7-9
Redwire Space	DIGITAL SUN SENSOR (±32°)	DIGITAL SUN SENSOR (±32°)	Sensor 0.3 kg Electronics ~1	1	Digital	±32° x ±32° (each sensor)	±0.1°	2	100	7-9
Redwire Space	Digital Sun Sensor (±64°)	Digital Sun Sensor (±64°)	Sensor0.25 Electronics 0.29 - 1.1	0.5	Digital	128° X 128° (EACH SENSOR) NOTE: 4π STERADIANS ACHIEVED WITH 5 SENSORS	±0.25°	2	100	7-9

Redwire Space	Fine Pointing Sun Sensor	Fine Pointing Sun Sensor	Sensor .95 Electronics 1.08	< 3	Digital	±4.25° x ±4.25° (Typical)	Better than ±0.01°	2	100	7-9
Redwire Space	Fine Spinning Sun Sensor (±64°)	Fine Spinning Sun Sensor (±64°)	Sensor 0.109 Electronics 0.475 – 0.725	0.5	Analog and Digital	±64° FAN SHAPED (each sensor)	±0.1°	1 plus Sun Pulse	100	7-9
Redwire Space	Micro Sun Sensor	Micro Sun Sensor	< 0.002	< 0.02	Analog	± 85° MINIMUM	±5°	2	Approx. 10	5-6
Redwire Space	Miniature Spinning Sun Sensor (±87.5°)	Miniature Spinning Sun Sensor (±87.5°)	<0.25	0.5	Digital	±87.5° (FROM NORMAL TO SPIN AXIS)	±0.1°	1 plus Sun Pulse	100	7-9
Redwire Space	FINE SUN SENSOR (±50°)	FINE SUN SENSOR (±50°)	Unk	Unk	Digital	Typically ±50 x ±50°	±0.01° TO ±0.05°	2	100, 150, or 300	7-9
Bradford Engineering	CoSS	Cosine	0.024	0	Analog	160° full cone	3°	1	40000	7-9
Bradford Engineering	CoSS-R	Cosine	0.015	0	Analog	180° full cone	3°	1	120000	7-9
Bradford Engineering	CSS-01, CSS-02	Cosine	0.215	0	Analog	180° full cone	1.5°	2	70000	7-9
Bradford Engineering	FSS	Quadrant	0.375	0.25	Analog	128° x 128°	0.3°	2	100	7-9
Bradford Engineering	Mini-FSS	Quadrant	0.050	0	Analog	128° x 128°	0.2°	2	20000	7-9
CubeSpace	CubeSense	Camera	0.030	0.2	Digital	170° full cone	0.2°	2	24	7-9
GomSpace	NanoSense FSS	Quadrant	0.002	Unk	Digital	{45°, 60°}	{±0.5°, ±2°}	2	Unk	Unk

Hyperion Technologies	SS200	Unk	.003	.04	Digital	110°	0.3°	Unk	36	7-9
Lens R&D	BiSon64-ET	Quadrant	0.023	0	Analog	±58° per axis	0.5°	2	9200	7-9
Lens R&D	BiSon64-ET-B	Quadrant	0.033	0	Analog	±58° per axis	0.5°	2	9200	7-9
Lens R&D	MAUS	Quadrant	0.014	0	Analog	±57° per axis	0.5°	2	9200	7-9
NewSpace Systems	NFSS-411	Unk	0.035	0.150	Digital	140°	0.1°	TBD	20	7-9
NewSpace Systems	NCSS-SA05	Unk	0.005	0.05	Analog	114°	0.5°	TBD	Unk	7-9
Solar MEMS Technologies	nanoSSOC-A60	Quadrant	0.004	0.007	Analog	±60° per axis	0.5°	2	100	7-9
Solar MEMS Technologies	nanoSSOC-D60	Quadrant	0.007	0.076	Digital	±60° per axis	0.5°	2	30	7-9
Solar MEMS Technologies	SSOC-A60	Quadrant	0.025	0.01	Analog	±60° per axis	0.3°	2	100	7-9
Solar MEMS Technologies	SSOC-D60	Quadrant	0.035	0.315	Digital	±60° per axis	0.3°	2	30	7-9
Solar MEMS Technologies	ACSS	Quadrant & Redundant	0.035	0.072	Analog	±60° per axis	0.5°	2	200	7-9
Space Micro	CSS-01, CSS-02	Cosine	0.010	0	Analog	120° full cone	5°	1	100	7-9
Space Micro	MSS-01	Quadrant	0.036	0	Analog	48° full cone	1°	2	100	7-9

5.2.8 Horizon Sensors

Horizon sensors can be simple infrared horizon crossing indicators (HCI), or more advanced thermopile sensors that can be used to detect temperature differences between the poles and equator. For terrestrial applications, these sensors are referred to as Earth Sensors, but can be used for other planets. Examples of such technologies are described in table 5-8 and illustrated in figure 5.6.

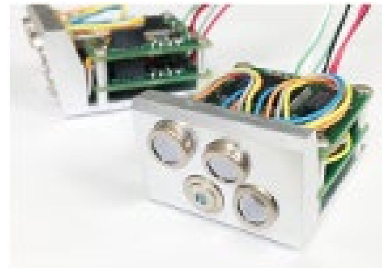

Figure 5.6: MAI-SES. Credit: Redwire Space

In addition to the commercially-available sensors listed in table 5-8, there has been some recent academic interest in horizon sensors for CubeSats with promising results (27) (10) (11).

Table 5-8. Commercially Available Horizon Sensors

Manufacturer	Model	Sensor Type	Mass (kg)	Peak Power (W)	Analog or Digital	Accuracy	# Measurement Angles	Rad Tolerance (krad)	TRL
CubeSpace	CubeSense	Camera	0.030	0.200	Digital	0.2°	2	24	7-9
CubeSpace	CubeIR	Infrared	0.050	0.230	Digital	1.5°	2	24	7-9
Servo	Mini Digital HCI	Pyroelectric	0.050	Voltage Dependent	Digital	0.75°	Unk	Unk	7-9
Servo	Mini HCI	Pyroelectric	0.0115	Voltage Dependent	Unk	Unk	Unk	Unk	Unk
Servo	RH 310 HCI	Pyroelectric	1.5	1	Unk	0.015°	Unk	20	Unk
Solar MEMS Technologies	HSNS	Infrared	0.120	0.150	Digital	1°	2	30	7-9

5.2.9 Inertial Sensing

Inertial sensing is a broad category which includes gyroscopes for measuring angular change and accelerometers for measuring velocity change.

Inertial sensors are packaged in different ways, ranging from single-axis devices (e.g., a single gyroscope or accelerometer), to packages which include multiple axes of a single device type (e.g., Inertial Reference Units are typically three gyroscopes mounted in a triad orientation to provide three-axes angular change), to Inertial Measurement Units (IMUs), which are packages which include multiple axes of both gyroscopes and accelerometers (to enable 6-DOF inertial propagation). Some vendors also offer packages that incorporate magnetometers and barometers.

Inertial sensors are frequently used to propagate the vehicle state between measurement updates of a non-inertial sensor. For example, star trackers typically provide attitude updates at 5 Hz or possibly 10 Hz. If the control system requires accurate knowledge between star tracker updates, then an IMU may be used for attitude propagation between star tracker updates.

The main gyroscope types used in modern small spacecraft are fiber optic gyros (FOGs) and MEMS gyros, with FOGs usually offering superior performance at a mass and cost penalty (12). Other gyroscope types exist (e.g., resonator gyros, ring laser gyros), but these are not common in the SmallSat/CubeSat world due to size, weight, and power (SWaP) and cost considerations.

Gyro behavior is a complex topic (13) and gyro performance is typically characterized by a multitude of parameters. Table 5-9 only includes bias stability and angle random walk for gyros, and bias stability and velocity random walk for accelerometers, as these are often the driving performance parameters. That said, when selecting inertial sensors, it is important to consider other factors such as dynamic range, output resolution, bias, sample rate, etc.

Table 5-9. Gyros Available for Small Spacecraft

Manufacturer	Model	Sensor Type	Technology	Mass (kg)	Power (W)	Gyros				Accelerometers			
							Bias Stability		ARW		Bias Stability		VRW
						# Axes	(°/hr)	stat	(°/rt(hr))	# Axes	(µg)	stat	(m/sec) /rt(hr)
Advanced Navigation	Orientus	IMU + magnetometers	MEMS	0.025	0.325	3	3.000	TBD	0.240	3	20	TBD	0.059
Advan Tech International	AU7684	IMU	MEMS	TBD	TBD	3	10.000	TBD	0.500	3	2000	TBD	TBD
Epson	M-G370	IMU	MEMS	0.010	0.016	3	0.800	av	0.060	3	12	av	0.025
Epson	M-G365	IMU	MEMS	0.010	0.016	3	1.200	av	0.080	3	16	av	0.033
Epson	M-G364	IMU	MEMS	0.010	TBD	3	2.200	av	0.090	3	50	av	0.025
Epson	M-G354	IMU	MEMS	0.010	TBD	3	3.000	av	0.100	3	70	av	0.030
Emcore	SDI50x-AF00	IMU	MEMS	0.60	5.0	3	1	1σ	0.02	3	100	1σ	0.059
Emcore	SDI50x-BF00	IMU	MEMS	0.60	5.0	3	3	1σ	0.02	3	200	1σ	0.059
Emcore	SDI50x-CF00	IMU	MEMS	0.60	5.0	3	10	1σ	0.02	3	200	1σ	0.071
Emcore	SDG500	Gyro	MEMS	0.025	0.6	1	20	Typical	N/A	N/A	N/A	N/A	N/A

Emcore	SDG1400	Gyro	MEMS	0.60	0.6	1	6	Typical	N/A	N/A	N/A	N/A	N/A
Emcore	SDD3000-A01	Gyro	MEMS	0.227	2.25	1	0.5	1σ	N/A	N/A	N/A	N/A	N/A
Emcore	QRS11	Gyro	MEMS	≤0.06	0.8	1	6	Typical	N/A	N/A	N/A	N/A	N/A
Emcore	QRS14-102	Gyro	MEMS	≤0.05	0.3	1	N/A	N/A	N/A	N/A	N/A	N/A	N/A
Emcore	QRS14-103	Gyro	MEMS	≤0.05	0.7	1	N/A	N/A	N/A	N/A	N/A	N/A	N/A
Emcore	QRS28	Gyro	MEMS	≤0.025	0.5	2	N/A	N/A	N/A	N/A	N/A	N/A	N/A
Emcore	QRS116	Gyro	MEMS	≤0.06	0.2	1	20	1σ	N/A	N/A	N/A	N/A	N/A
Emcore	EN-300-1	IMU	FOG	0.82	18.0	3	0.1	1σ	0.008	3	150	1σ	0.026
Emcore	EN-300-3	IMU	FOG	0.82	18.0	3	0.2	1σ	0.015	3	300	1σ	0.026
Emcore	EN-300-5	IMU	FOG	0.82	18.0	3	0.4	1σ	0.03	3	500	1σ	0.026
Emcore	EG-120	Gyro	FOG	0.08	5.0	1	1	1σ	≤0.04	N/A	N/A	N/A	N/A
Gladiator Technologies	A40	Accel	MEMS	0.015	TBD	0	N/A	Unk	N/A	1	45	TBD	0.038
Gladiator Technologies	G150Z	Gyro	MEMS	0.028	TBD	1	1.200	TBD	0.060	0	N/A	N/A	N/A
Gladiator	G300D	IRU	MEMS	0.019	0.25	3	5.000	TBD	0.168	0	N/A	N/A	N/A

Technologies													
Gladiator Technologies	LandMark 60LX	IMU	MEMS	0.115	0.600	3	4.000	TBD	0.096	3	10	TBD	0.0016
Gladiator Technologies	LandMark 005	IMU	MEMS	0.019	0.400	3	3.5	TBD	0.102	3	20	TBD	0.0024
Gladiator Technologies	LandMark 007	IMU	MEMS	0.025	0.270	3	4.000	TBD	0.12	3	5000	TBD	0.3
Gladiator Technologies	LandMark 007X	IMU	MEMS	0.025	0.450	3	4.000	TBD	0.12	3	5000	TBD	0.3
Gladiator Technologies	LandMark 60LX	IMU	MEMS	0.115	0.600	3	4.000	TBD	0.096	3	10	TBD	0.00168
Gladiator Technologies	LandMark 65	IMU	MEMS	0.115	0.600	3	7.000	TBD	0.120	3	10	TBD	0.0021
Gladiator Techn	MRM60	IMU	MEMS	0.120	1.000	3	3.000	TBD	0.096	3	25	TBD	0.0024

ologies													
Honeywell	MIMU	IMU	RLG	Unk	Unk	Unk	Unk	Unk	Unk	Unk	Unk	Unk	Unk
Honeywell	HG1930	IMU	MEMS	0.16	3.000	3	20.000	1σ	0.175	3	10	1σ	0.400
Honeywell	HG1700	IMU	RLG	0.9	5.000	3	1.000	1σ	0.125	3	1000	1σ	0.65
Inertial Sense	μIMU	IMU + magnetometers +barometer	MEMS	0.011	0.340	3	10.000	max	0.150	3	40	max	0.070
Inertial Labs	IMU-NAV-100 "Tactical" A	IMU	MEMS	0.155	0.800	3	0.500	rms	0.100	3	3	rms	0.008
Inertial Labs	IMU-P "Tactical" Standard A	IMU	MEMS	0.070	0.800	3	1.000	rms	0.200	3	5	rms	0.015
KVH	1725 IMU	IMU	FOG	0.700	8.000	3	0.10	1σ	0.017	3	15	1σ	0.071
KVH	1750 IMU	IMU	FOG	0.700	8.000	3	0.100	1σ	0.012	3	45	1σ	0.014
KVH	1775 IMU	IMU + magnetometers	FOG	0.700	8.000	3	0.100	1σ	0.012	3	45	1σ	0.071
KVH	CG-5100	IMU	FOG	2.270	15.000	3	1	1σ	0.067	3	250	1σ	0.12
KVH	DSP-1760	IRU	FOG	0.600	8.000	3	0.100	1σ	0.0120	0	N/A	Unk	N/A

KVH	DSP-3000	Gyro	FOG	0.270	3.000	1	1.000	1σ	0.067	0	N/A	Unk	N/A
KVH	DSP-3100	Gyro	FOG	0.200	3.000	1	1.000	1σ	0.067	0	N/A	Unk	N/A
KVH	DSP-3400	Gyro	FOG	0.300	3.000	1	1.000	1σ	0.067	0	N/A	Unk	N/A
KVH	DSP-4000	Gyros	FOG	2.360	9.000	2	1.000	1σ	0.067	0	N/A	Unk	N/A
L3	CIRUS	Gyros	FOG	15.400	40.000	3	0.000	1σ	0.100	0	N/A	Unk	N/A
LORD Sensing	3DM-CV5-10	IMU	MEMS	0.011	0.500	3	8.000	TBD	0.450	3	80	TBD	0.059
LORD Sensing	3DM-CX5-10	IMU	MEMS	0.008	0.300	3	8.000	TBD	0.300	3	40	TBD	0.015
LORD Sensing	3DM-GX5-10	IMU	MEMS	0.0165	0.300	3	8.000	TBD	0.300	3	40	TBD	0.015
MEMSENSE	MS-IMU3020	IMU + magnetometer	MEMS	0.020	0.650	3	1.060	typ	0.220	3	14.8	typ	0.078
MEMSENSE	MS-IMU3025	IMU + magnetometer	MEMS	0.019	0.850	3	0.80	typ	0.150	3	6.7	typ	0.008
MEMSENSE	MS-IMU3030	IMU + magnetometer	MEMS	0.025	1.350	3	0.550	typ	0.11	3	2.9	typ	0.005

MEMSENSE	MS-IMU3050	IMU + magnetometer	MEMS	0.079	2.500	3	0.300	typ	0.065	3	2.6	typ	0.006
NewSpace Systems	NSGY-001	IRU	Image-based rotation estimate	0.055	0.200	3	N/A		N/A	0	N/A	Unk	N/A
Northrop Grumman	LN-200S	IMU	FOG, SiAc	0.748	12	3	1.000	1σ	0.070	3	300	1σ	Unk
Northrop Grumman	μFORS-3U	Gyro	FOG	0.150	2.300	1	0.050	1σ	0.080	0	N/A	Unk	N/A
Northrop Grumman	μFORS-6U	Gyro	FOG	0.150	2.300	1	0.050	1σ	0.047	0	N/A	Unk	N/A
Northrop Grumman	μFORS-36m	Gyro	FOG	0.110	2.25	1	18.000	1σ	1.000	0	N/A	Unk	N/A
Northrop Grumman	μFORS-1	Gyro	FOG	0.137	2.5	1	1.000	1σ	0.100	0	N/A	Unk	N/A
Northrop Grumman	μIMU-I-SP	IMU	MEMS	0.680	8.000	3	6.000	1σ	0.300	3	3000	rms	0.147
Northrop Grumman	μIMU-I-HP	IMU	MEMS	0.680	8.000	3	3.000	1σ	0.150	3	1500	rms	0.041

Northrop Grumman	μIMU-IC-SP	IMU	MEMS	0.680	8.000	3	6.000	1σ	0.300	3	3000	rms	0.147
Northrop Grumman	μIMU-IC-HP	IMU	MEMS	0.680	8.000	3	9.000	1σ	0.150	3	1500	rms	0.041
Northrop Grumman	μIMU-M-SP	IMU	MEMS	0.680	8.000	3	9.000	1σ	0.450	3	3000	rms	0.147
Northrop Grumman	μIMU-M-HP	IMU	MEMS	0.680	8.000	3	4.500	1σ	0.230	3	1500	rms	0.041
NovAtel	IMU-HG1900	IMU	MEMS	2.500	8.000	3	1.000	TBD	0.090	3	700	TBD	Unk
NovAtel	IMU-μIMU-IC	IMU	MEMS	2.570	11.000	3	6.000	TBD	0.300	3	3000	TBD	0.250
NovAtel	OEM-IMU-ADIS-16488	IMU	MEMS	0.048	0.254	3	6.25	TBD	0.300	3	100	TBD	0.029
NovAtel	OEM-IMU-EG370N	IMU	MEMS	0.010	0.100	3	0.800	TBD	0.060	3	12	TBD	0.025
NovAtel	OEM-HG1900	IMU	MEMS	0.460	3.000	3	1.000	TBD	0.090	3	700	TBD	Unk
NovAtel	OEM-HG1930	IMU	MEMS	0.200	3.000	3	2.000	TBD	0.125	3	3000	TBD	Unk

NovAtel	OEM-IMU-HG4930P	IMU	MEMS	0.200	3.000	3	Unk	TBD	Unk	3	Unk	TBD	Unk
NovAtel	OEM-IMU-STIM300	IMU	MEMS	0.055	1.50	3	0.500	TBD	0.150	3	50	TBD	0.060
Sensonor	STIM202	IRU	MEMS	0.055	1.500	3	0.400	TBD	0.170	0	N/A	TBD	N/A
Sensonor	STIM210	IRU	MEMS	0.052	1.500	3	0.300	TBD	0.150	0	N/A	TBD	N/A
Sensonor	STIM300	IMU	MEMS	0.055	2.000	3	0.300	TBD	0.150	3	50	TBD	0.070
Sensonor	STIM318	IMU	MEMS	0.057	2.500	3	0.300	TBD	0.150	3	3	TBD	0.015
Sensonor	STIM320	IMU	MEMS	0.057	2.500	3	0.300	TBD	0.100	3	3	TBD	0.015
Sensonor	STIM277H	IRU	MEMS	0.052	1.500	3	0.300	TBD	0.150	0	N/A	TBD	N/A
Sensonor	STIM377H	IMU	MEMS	0.055	2.000	3	0.300	TBD	0.150	3	50	TBD	0.070
Silicon Sensing Systems	CRH03	Gyro	MEMS	0.42	0.2 W	1	CRH03-010 – 0.03 CRH03-025 – 0.04 CRH03-100 – 0.04		CRH03-010 – 0.005 CRH03-025 – 0.006 CRH03-100 – 0.006	0	N/A	-	N/A

							CRH03-200 – 0.05 CRH03-400 – 0.1		CRH03-200 – 0.008 CRH03-400 – 0.010				
Silicon Sensing Systems	CRH03 (OEM)	Gyro	MEMS	0.18	0.2 W	1	CRH03-010 – 0.03 CRH03-025 – 0.04 CRH03-100 – 0.04 CRH03-200 – 0.05 CRH03-400 – 0.1		CRH03-010 – 0.005 CRH03-025 – 0.006 CRH03-100 – 0.006 CRH03-200 – 0.008 CRH03-400 – 0.010	0	N/A	-	N/A
Silicon Sensing Systems	RPU30	Gyro	MEMS	1.35	<0.8 W	3	0.06		0.006	0	N/A	-	N/A
Silicon Sensing Systems	DMU41	9 DoF IMU	MEMS	<2	<1.5 W	3	0.1		0.015	3	15	-	0.05
Silicon Sensing Systems	DMU11	6 DoF IMU	MEMS	0.04	0.425	3	10		0.4	3	50	-	0.05

Silicon Sensing Systems	CRM	Gyro	MEMS	0.001	0.0165	1	12		0.2	0	N/A		N/A
Silicon Sensing Systems	CAS	Acc	MEMS	0.004	Unk	0	N/A		N/A	2	CAS2X 1S - 7.5 CAS2X 2S - 7.5 CAS2X 3S - 7.5 CAS2X 4S - 25 CAS2X 5S - 75		CAS2X 1S - TBC CAS2X 2S - TBC CAS2X 3S - TBC CAS2X 4S - TBC CAS2X 5S - TBC
Systron Donner	SDI50x-AE00	IMU	MEMS	0.590	5.000	3	1.000	1σ	0.020	3	100	1σ	0.059
Thales	InterSense NavChip Series 3 Class A	IMU	MEMS	0.003	0.135	3	4.000	TBD	0.180	3	6	TBD	0.020
Thales	InterSense NavChip Series 3 Class B	IMU	MEMS	0.003	0.135	3	5.000	TBD	0.180	3	40	TBD	0.030
Thales	InterSense NavChip	IMU	MEMS	0.003	0.135	3	5.000	TBD	0.180	3	40	TBD	0.030
Thales	InterSense InertiaCube4	IRU	MEMS	0.011	TBD	3	TBD	TBD	TBD	0	N/A	Unk	N/A

Vector Nav	VN-100	IMU + magnetometers +barometer	MEMS	0.015	0.220	3	10.000	max	0.210	3	40	max	0.082
Vector Nav	VN-110	IMU + magnetometers	MEMS	0.125	2.500	3	1.000	max	0.054	3	10	max	0.024
Xsens Technologies	MTi-610	IMU	MEMS	0.009	1.0	3	8.000	TBD	0.420	3	10	TBD	0.035

5.2.10 GPS Receivers

For low-Earth orbit spacecraft, GPS receivers are now the primary method for performing orbit determination, replacing ground-based tracking methods. Onboard GPS receivers are now considered a mature technology for small spacecraft, and some examples are described in table 5-10. There are also next-generation chip-size COTS GPS solutions, for example the NovaTel OEM 719 board has replaced the ubiquitous OEMV1.

GPS accuracy is limited by propagation variance through the exosphere and the underlying precision of the civilian use C/A code (14). GPS units are controlled under the Export Administration Regulations (EAR) and must be licensed to remove Coordinating Committee for Multilateral Export Control (COCOM) limits (15).

However, past experiments have demonstrated the ability of using a weak GPS signal at GSO, and potentially soon to cislunar distances (16) (17). Development and testing in this fast-growing area of research and development may soon make onboard GPS receivers more commonly available.

Table 5-10. GPS Receivers for Small Spacecraft

Manufacturer	Model	Mass (kg)	Power (W)	Accuracy (m)	Radiation Tolerance (krad)	TRL
APL	Frontier Radio Lite	0.4	1.3	15	20	5-6
Eurotech	COM-1289	0.85	3.625	1.2	Unk	Unk
General Dynamics	Explorer	1.2	8	15	100	7-9
General Dynamics	Viceroy-4	1.1	8	15	100	7-9
NASA GSFC	NavCube Mini 3.0 (Above GPS Constellation Receiver)	2.1*	11*	<80 @ 29Re** <30 @ Moon***	100	5-6
Novatel	OEM719	0.031	1.8	1.5	Unk	7-9
Novatel	OEM729	0.048	1.8	1.5	Unk	7-9
SkyFox Labs	piNAV-NG	0.024	0.124	10	30	7-9
SkyFox Labs	piPATCH-L1E1	0.05	0.02	Unk	Unk	7-9
SkyFox Labs	piPATCH-L1G1	0.05	0.02	Unk	Unk	7-9
SkyFox Labs	miniPATCH-L1	0.05	0.02	Unk	Unk	7-9
Surrey Satellite Technology	SGR-Ligo	0.09	0.5	5	5	5-6
GomSpace	GPS-kit	0.031	1.3	1.5	Unk	Unk

* Estimate does not include filter, LNA and antenna which will depend on the orbit
** About ½ way to the Moon with Ultra Stable Oscillator (not included in mass and power estimates)
*** With Rubidium Atomic Frequency Standard Clock (not included in mass and power estimates)

5.2.11 Deep Space Navigation

In deep space, navigation is performed using radio transponders in conjunction with the Deep Space Network (DSN). As of 2020, the only deep space transponder with flight heritage suitable for small spacecraft was the JPL-designed and General Dynamics-manufactured Small Deep Space Transponder (SDST). JPL has also designed IRIS V2, which is a deep space transponder that is more suitable for the CubeSat form factor. Table 5-11 details these two radios, and the SDST is illustrated in figure 5.7. IRIS V2, derived from the Low Mass Radio Science Transponder (LMRST), flew on the MarCO CubeSats and is scheduled to fly on INSPIRE (18) and was selected for seven Artemis I secondary payloads (28).

Figure 5.7: General Dynamics SDST. Credit: General Dynamics.

Table 5-11. Deep Space Transponders for Small Spacecraft

Manufacturer	Model	Mass (kg)	Power (W)	Bands	Radiation Tolerance (krad)	TRL
General Dynamics	SDST	3.2	19.5	X, Ka	50	7-9
Space Dynamics Laboratory	IRIS V2.1	1.2	35	X, Ka, S, UHF	15	7-9

5.2.12 Atomic Clocks

Atomic clocks have been used on larger spacecraft in low-Earth orbit for several years now, however integrating them on small spacecraft is relatively new. The conventional method for spacecraft navigation is a two-way tracking system of ground-based antennas and atomic clocks. The time difference from a ground station sending a signal and the spacecraft receiving the response can be used to determine the spacecraft's location, velocity, and (using multiple signals) the flight path. This is not a very efficient process, as the spacecraft must wait for navigation commands from the ground station instead of making real-time decisions, and the ground station can only track one spacecraft at a time, as it must wait for the spacecraft to return a signal (19). In deep space navigation, the distances are much greater from the ground station to spacecraft, and the accuracy of the radio signals needs to be measured within a few nanoseconds.

JPL's Deep Space Atomic Clock (DSAC) project plans to launch a prototype of a miniaturized, low-mass (16 kg) atomic clock based on mercury-ion trap technology which underwent demonstration testing in the fall of 2017. The project aims to produce a <10 kg configuration in the second generation. The DSAC was launched in 2019 as a hosted payload on General Atomics Orbital Test Bed spacecraft aboard the U.S. Air Force Space Technology Program (STP-2) mission (20), and has been extended for in-orbit demonstration through August 2021 and was still in orbit as of June 2021 (29).

More small spacecraft designers are developing their own version of atomic clocks and oscillators that are stable and properly synchronized for use in space. They are designed to fit small spacecraft, for missions that are power- and volume-limited or require multiple radios.

Table 5-12. Atomic Clocks and Oscillators for Small Spacecraft							
Manufacturer	**Model**	**Dimensions (mm)**	**Mass (kg)**	**Power (W)**	**Frequency Range**	**Rad Tolerance**	**TRL**
AccuBeat	Ultra Stable Oscillator	131 x 167 x 107	2	5.64 W	57.5185 MHz	50	7-9
Bliley Technologies	Miniature Half-DIP Package Low Power OCXO	Up to 12 x 12 x 10	0.01	0.180	10 MHz to 60 MHz	Unk	7-9
Bliley Technologies	Iris Series 1"x1" OCXO for LEO	19 x 11 x 19	0.016	1.5	10 MHz to 100 MHz	39	7-9
Bliley Technologies	Aether Series TCVCXO for LEO	21 x 14 x 8	Unk	0.056	10MHz to 150 MHz	37	Unk
Microsemi	Miniature Atomic Clock (MAC SA5x)	51 x 51 x 18	0.1	8	10 MHz	Unk	Unk
Microsemi	Space Chip Scale Atomic Clock (CSAC)	41 x 36 x 12	0.035	0.12	10 MHz	20	5-6

5.3 On the Horizon

Figure 5.8: High-speed magnetically levitated reaction wheel. Credit: Celeroton AG.

Technological progress in the area of guidance, navigation, and control is slow. Given the high maturity of existing GNC components, future developments in GNC are mostly focused on incremental or evolutionary improvements, such as decreases in mass and power, and increases in longevity and/or accuracy. This is especially true for GNC components designed for deep space missions, where small spacecraft missions have only very recently been demonstrated. However, in a collaborative effort between the Swiss Federal Institute of Technology and Celeroton, there is progress being made on a high-speed magnetically levitated reaction wheel for small satellites (figure 5.8). The idea is to eliminate mechanical wear and stiction by using magnetic bearings rather than ball bearings. The reaction wheel implements a dual hetero/homopolar, slotless, self-bearing, permanent-magnet synchronous motor (PMSM). The fully active, Lorentz-type magnetic bearing consists of a heteropolar self-bearing motor that applies motor torque and radial forces on one side of the rotor's axis, and a homopolar machine that exerts axial and radial forces to allow active control of all six degrees of freedom. It is capable of storing 0.01 Nm of momentum at a maximum of 30,000 rpm, applying a maximum torque of 0.01 Nm (21).

Another interesting approach to measuring angular velocity is the Stellar Gyro from NewSpace Systems. This sensor estimates angular rates from star images taken by a camera; one advantage of this approach is that it avoids the problem of gyro drift. Of course, such a sensor does require a clear view of the sky.

5.4 Summary

Small spacecraft GNC is a mature area, with many previously flown, high TRL components offered by several different vendors. Progress in developing integrated units will offer simple, single vendor, modular devices for ADCS, which will simplify GNC subsystem design. Other areas of GNC have potential for additional improvements as more research is being conducted. For example, a team at the University of Michigan is developing a multi-algorithmic hybrid ADCS system for CubeSats that can implement multiple estimation and control algorithms (22). Another team from Johns Hopkins University is conducting ground simulations of docking, charging, relative navigation, and deorbiting for a fully robotic CubeSat (23).

The rising popularity of SmallSats in general, and CubeSats in particular, means there is a high demand for components, and engineers are often faced with prohibitive prices. The Space Systems Design Studio at Cornell University is tackling this issue for GNC with their PAN nanosatellites. A paper by Choueiri et al. outlines an inexpensive and easy-to-assemble solution for keeping the ADCS system below $2,500 (25). Lowering the cost of components holds exciting implications for the future and will likely lead to a burgeoning of the SmallSat industry.

For feedback solicitation, please email: arc-sst-soa@mail.nasa.gov. Please include a business email so someone may contact you further.

References

(1) Shepherd, L. C. G. and Shepherd, A. F. S. C.: *“Space Surveillance Network.”* Shared Space Situational Awareness Conference. Olorado Springs. 2006.

(2) Vallado, D A, et al.: *“Revisiting spacetrack report 3."* 2006.

(3) Thornton, C L and Border, J S: "*Radiometric Tracking Techniques For Deep-Space Navigation."* s.l. : John Wiley & Sons,, 2003.

(4) JPL. MarCO: Mission Overview. *CubeSat.* [Online] 2020. [https://www.jpl.nasa.gov/CubeSat/missions/marco.php.

(5) Wertz, J. R.: "*Spacecraft attitude determination and control."* Springer Science & Business Media. *Vol. 73.* 2012,

(6) Jin, J, Ko, S and Ryoo, C K: *“Fault Tolerant Control For Satellites With Four Reaction Wheels.”* vol. 16, no. 10, pp. 1250–1258. 2008.

(7) Kulczycki, R. and Wisniewski, P.: *“Slew Maneuver Control For Spacecraft Equipped With Star Camera And Reaction Wheels.”* Vol. 13, no. 3, pp. 349–356. 2005.

(8) Spratling, B. B. and Mortari, D.: *“A Survey On Star Identification Algorithms.”* Vol. 2, no. 1, pp. 93–107. 2009.

(9) Psiaki, M L, Martel, F and Pal, P K.: *“Three-Axis Attitude Determination Via Kalman Filtering Of Magnetometer Data.”* Vol. 13, no. 3, pp. 506–514. 1990.

(10) Wessels, J H.: "Infrared Horizon Sensor for CubeSat Implementation." *Masters Thesis, Stellenbosch University.* 03 2018.

(11) Pelemeshko, A, et al.: "*High-Precision Cubesat Sun Sensor Coupled With Infrared Earth Horizon Detector."* IOP Conf. Ser.: Mater. Sci. Eng. Vol. 734. pp. 0121-8. 2020,

(12) Greenheck, D, et al.: *"Design and Testing of a Low-Cost MEMS IMU Cluster for SmallSat Applications."* 2014. 28th Annual AIAA/USU Conference on Small Satellites.

(13) Merhav, S.: *Aerospace Sensor Systems and Applications.* Springer New York, 1998.

(14) Montenbruck, O. et al.: *"Precision Spacecraft Navigation Using A Low-Cost GPS Receiver."* Vol. 16, no. 4, pp. 519–529. 2014.

(15) *"Foreign Availability Determination Procedures And Criteria."* Office of the Federal Register. Title 15 Part 768.7. 2015.

(16) Jeffery Foust: "GPS in Space." *MIT Technology Review.* [Online] 01 2002. https://www.technologyreview.com/2002/01/01/275613/gps-in-space/.

(17) Adam Hadhazy: "Cosmic GPS." *Aerospace America.* [Online] 05 2020. https://aerospaceamerica.aiaa.org/features/cosmic-gps/.

(18) Aguirre, F. H.: *"X-Band Electronics For The INSPIRE Cubesat Deep Space Radio."* 2015. IEEE Aerospace Conference.

(19) Baird, D.: "NASA Tests Atomic Clock for Deep Space Navigation." [Online] 2018. https://www.jpl.nasa.gov/news/news.php?feature=7053.

(20) Cornwell, D.: "NASA's Deep Space Atomic Clock and Optical Communications Program for PNT Applications." [Online] 2016. [Cited: June 19, 2018.] https://www.gps.gov/governance/advisory/meetings/2016-12/cornwell.pdf.

(21) JW, Kolar, et al.: "*High-Speed Magnetically Levitated Reaction Wheels For Small Satellites."* Anacapri, Capri: 23rd International Symposium on Power Electronics, Electrical Drives, Automation and Motion (SPEEDAM 2016), 2016.

(22) Lee, D Y, Kuevor, P. and Culter, J.: "Multi-algorithmic Hybrid Attitude Determination and Control System of the CubeSat 'CADRE'." [Online] 2016. https://digitalcommons.usu.edu/smallsat/2016/S2CDH/2/.

(23) Mishra, S., Basescu, M. and Kobilarov, M.: "Laboratory Validation of Vision Based Grasping, Guidance and Control with Two Nanosatellite Models." [Online] 2016. https://digitalcommons.usu.edu/smallsat/2016/S5GuidCont/6/.

(24) Gunter, B. C., et al.: "The Ranging and Nanosatellite Guidance Experiment (RANGE)." [Online] 2016. https://digitalcommons.usu.edu/smallsat/2016/S5GuidCont/3/.

(25) Choueiri, M N, Bell, M and Peck, M A.: "Cost-Effective and Readily Manufactured Attitude Determination and Control System for NanoSatellites." *AIAA/ASCE/AHS/ASC Structures, Structural Dynamics, and Materials Conference, AIAA SciTech Forum.* 2018.

(26) D. Dickinson: “NICER and SEXTANT demonstrate XNAV pulsar navigation system that may be used on Artemis.” [Online] 2020. https://skyandtelescope.org/astronomy-news/nasa-to-use-pulsar-navigation-for-deep-space-missions/

(27) Kapás, K., Bozóki, T., Dálya, G. et al. Attitude determination for nano-satellites – I. Spherical projections for large field of view infrasensors. Exp Astron 51, 515–527 (2021). https://doi.org/10.1007/s10686-021-09730-y

(28) M. M. Kobayashi et al., "The Iris Deep-Space Transponder for the SLS EM-1 Secondary Payloads," in IEEE Aerospace and Electronic Systems Magazine, vol. 34, no. 9, pp. 34-44, 1 Sept. 2019, doi: 10.1109/MAES.2019.2905923.

(29) NASA: “Deep Space Atomic Clock.” [Online] 2021 https://www.jpl.nasa.gov/missions/deep-space-atomic-clock-dsac